Desalination and Water Treatment
www.deswater.com
doi: 10.1080/19443994.2016.1159250

57 (2016) 25991–26002
November

Taylor & Francis
Taylor & Francis Group

Treatment of truck wash water using electrocoagulation

Andrew J. Gomes[a,*], Kamol K. Das[b], Sadia A. Jame[b], David L. Cocke[a]

[a]*Department of Chemical Engineering, Lamar University, 4400 MLK Parkway, Beaumont, TX 77710, USA, Tel. +409 880 7974; Fax: +409 880 8270; email: andrew.gomes@lamar.edu (A.J. Gomes), Tel. +409 880 8750; email: deltagco@hotmail.com (D.L. Cocke)*
[b]*Department of Civil Engineering, Lamar University, 4400 MLK Parkway, Beaumont, TX 77710, USA, Tel. +765 998 1341; email: kamoldas@yahoo.com (K.K. Das), Tel. +409 499 7066; email: sarin301@yahoo.com (S.A. Jame)*

Received 27 May 2014; Accepted 23 February 2016

ABSTRACT

The scarcity of fresh water resources and the need for additional water supplies are critical in many regions of the world. Treatment of wastewater and its reuse can partially resolve this issue. Due to the increase in use and number of heavy duty vehicles for transportation purpose the wastewater generated from truck wash has been escalated during last several decades. Our results show that electrocoagulation (EC) can be an effective technique to treat truck wash water (TWW), and this treated TWW is reusable. Effects of different combination of electrodes, such as Fe–Fe, Al–Fe, and Al–Al, operating time, current density (CD), and pH inside the EC reactor were studied to optimize treatment conditions for lowering chemical oxygen demand (COD), and concentrations of some selected toxic metal ions in TWW. The best removal efficiency of 79% for COD was obtained by Fe–Fe combination after 8 min of operating time and at 2 mA/cm^2 of CD. Iron, zinc, and lead concentrations were reduced below EPA maximum contaminant levels for all three types of electrode combinations. The EC-floc was characterized using X-ray diffraction, scanning electron microscope/energy dispersive X-ray spectroscopy, and Fourier transform-infrared spectrometer. The ionic substitution of iron by aluminum was confirmed in the isomorphs subsisted in the floc.

Keywords: Truck wash water; Electrocoagulation; COD; Lead; Iron; Zinc; Reuse

1. Introduction

Increasing human demand exerts increasing pressure on the environment. The pressure results significant impact that vary from the ambient milieu distortion to global environmental pollution unless the treatment processes are performed. In some cases, reuse of the environmental resource imparts less pressure on the local environment. The increasing population requires greater number of transportation units to meet their daily demand. According to US census 2010 data, a large amount of water is used daily to wash over 7,083,000 trucks in USA with 6,790,882 single-unit 2-axle 6-tire vehicles and 22,15,856 other combination trucks [1]. Trucks are used for the faster transfer of the daily goods among the states. These trucks necessitate washing frequently rendering polluted wash water containing several harmful components such as oil, grease, heavy metals, and detergents remnants [2–4].

Several processes exist to treat effluent wastewater as well as fleet wash water such as coagulation,

*Corresponding author.

1944-3994/1944-3986 © 2016 Balaban Desalination Publications. All rights reserved.

membrane filtration, reverse osmosis, electrooxidation, electrofenton, and finally electrocoagulation (EC) [5–13]. Among all the existing treatment technologies, EC received significant focus because of its simplicity, cost-effectiveness, ease for establishment, and less production of byproducts [14]. EC can be vastly used for the treatment of effluent from food and oil processing industries, tanneries, textile, pulp and paper, poultry processing, and produced water [15–19]. The EC has been successfully used to treat oil wastes, with a removal efficiencies as high as 99%. A similar success was obtained when treating dye-containing solutions, potable water, urban and restaurant wastewater, and nitrate or fluoride containing waters [20–26]. In addition, a great deal of work performed in the last decades has proved that EC is an effective technology for the treatment of heavy metal containing solutions. It is moderately effective in reducing chemical oxygen demand (COD) of the effluent water [27].

In EC, the flocculating agent is generated by electro-oxidation of a sacrificial anode, generally made of iron or aluminum. In this process, the treatment is performed without adding any chemical coagulant or flocculant, hence reducing the amount of sludge, which must be disposed. Since, reclamation has attracted more attention in the past several years from regulators and manufacturers as a means of water conservation and quality control [28–32], our research goal was to treat truck wash water (TWW) by EC in order to reduce the contaminants amount below the EPA maximum contaminant levels (MCL). This way, the treated water can be simply reused for the same purpose in the same facility as schematically shown in Fig. 1. Consequently, the discharge load will be decreased, and the cost-effectiveness will be increased.

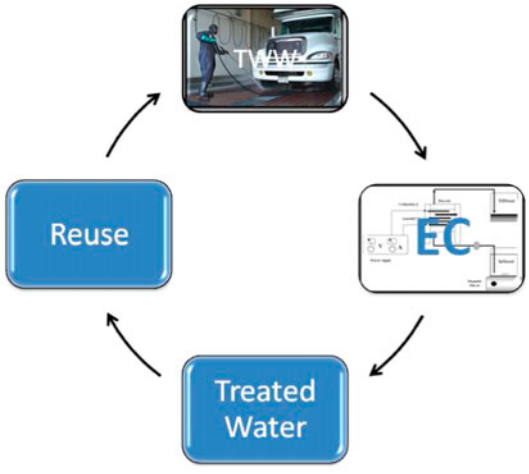


Fig. 1. The scheme for reuse of TWW after treatment with EC.

1.1. Reactions in EC

EC consists of an in situ generation of coagulants formed by electrical dissolution of iron or aluminum electrodes. The generation of metallic cations takes place at the anode, whereas typically hydrogen is produced at the cathode. The generated gas helps the flotation of flocculated particles, and therefore the process is additionally associated to electroflocculation. The electrodes can be arranged either as monopolar or bipolar when multiple electrodes are used.

Generally, at the anode, the metal gets oxidized to its cationic form. Such as, iron is converted to Fe^{2+}, or Fe^{3+}, and aluminum is converted to Al^{3+}. Further oxidation of Fe^{2+} can also take place at the anode by the presence of other oxidants or dissolved oxygen in aqueous phase [21]:

$$O_2 + 4Fe^{2+} + 4H^+ \rightarrow 4Fe^{3+} + 2H_2O \text{ (in acidic solution)} \quad (1)$$

$$O_2 + 4Fe^{2+} + 2H_2O + 8OH^- \rightarrow 4Fe(OH)_3 \text{ (in alkaline solution)} \quad (2)$$

In aqueous solutions of pH > 13, ferric-hydroxo complex, $Fe(OH)_4^-$ is formed [33]:

$$4Fe(OH)_3 + 4OH^- \rightarrow 4Fe(OH)_4^- \quad (3)$$

Fe^{3+} can be hydrolyzed to $Fe(OH)_2^+$. According to the theoretical study of Abreu et al. [34], the hydrated form of $Fe(OH)_2^+$ was found to be the most stable species among Fe(III) hydrolysis products.

$$Fe^{3+} + H_2O \rightarrow Fe(OH)^{2+} + H^+ \quad (4)$$

$$Fe(OH)^{2+} + H_2O \rightarrow Fe(OH)_2^{1+} + H^+ \quad (5)$$

$$Fe(OH)_2^{1+} + H_2O \rightarrow Fe(OH)_3 + H^+ \quad (6)$$

At the cathode, water is either reduced to hydrogen and hydroxides ions as found in alkaline solutions, or hydroxonium ions are reduced to hydrogen gas and water as observed in acidic solutions:

$$2H_2O + 2e^- \rightarrow H_2 + 2OH^- \text{ (in alkaline solution)} \quad (7)$$

$$2H_3O^+ + 2e^- \rightarrow H_2 + 2H_2O \text{ (inacidic solution)} \quad (8)$$

Typically during EC the pH of the solution near the cathode increases with time. Electrophoretic force

causes OH^- ion to migrate to the anode, so the pH near the anode becomes higher than in the bulk solution, thus favoring the formation of ferric hydroxide or aluminum hydroxide [35]:

$$Fe^{3+} + 3OH^- \rightarrow Fe(OH)_3 \quad (9)$$

$$Al^{3+} + 3OH^- \rightarrow Al(OH)_3 \quad (10)$$

If the anode potential is sufficiently high, secondary reactions may occur at the anode, such as direct oxidation of organic compounds, H_2O or Cl^- present in wastewater:

$$2Cl^- \rightarrow Cl_2 + 2e^- \quad (11)$$

$$2H_2O \rightarrow O_2 + 4H^+ + 4e^- \quad (12)$$

1.2. Green rust formation

When iron sacrificial electrodes are used, green rust (GR) is formed as intermediate materials. GR is layered double hydroxides, having pyroaurite-type structures. This structure consists of alternating positively charged hydroxide layers and hydrated anions in interlayers. In the structure, some of Fe(II) ions of the octahedral sheets of $Fe(OH)_2$ are replaced by Fe (III). Studies show that GR conforms to a general chemical composition and stoichiometry that can be represented with the following general formula [36]:

$$[Fe^{II}_{(6-x)}Fe^{III}_x(OH)_{12}]^{x+}[(A)_{x/n}\ yH_2O]^{x-} \quad (13)$$

where x ranges from 0.9 to 4.2, A is an n-valent anion (typically CO_3^{2-}, Cl^- or SO_4^{2-} and y denotes the varying amounts of interlayer water (typically ranges from 2 to 4 for most GR). Depending on types of anions, the mineral structures of GR can be rhombic obtained with "planar" anions such as chlorides, carbonate, etc. or hexagonal obtained with three-dimensional tetrahedral anions such as sulfate or selenate [37]. We assume that the presence of exchangeable cations and anions, and the interlayers in GR are responsible for removal of metals and other organic/inorganic species from wastewater when it is treated with EC.

2. Experimental

TWW was collected in plastic tank from nearby truck washing centers of Beaumont, Texas. Sample was preserved in 23°C according to the standard water sampling methods [38]. TWW was treated using two types of EC reactors: batch reactor, and flow-through EC apparatus (FTECA).

2.1. Batch reactor

Three combinations of electrodes were used for the experiments: Fe–Fe, Al–Fe, and Al–Al. There are several studies in the literature where better removal efficiency of water contaminants using Al–Fe electrode pairs was reported [39–42]. Batch EC experiments were carried out in a beaker with 400 mL solution using vertically positioned electrodes dipped in the solution. The anode and cathode were with dimensions of 3.2 × 6.2 cm, both electrodes having a submerged surface area of 14.4 cm^2. The electrode spacing was 2.5 cm. Electrodes were connected to a DC power supply (Kaselco power supply). EC batch experiments were performed at a constant current of 0.2 A at 50 V. A digital multimeter was used to measure the cell voltage. The polarity of the electrodes was changed after every minute of EC run to minimize the possibility of passivation on the electrodes.

EC batch experiments were run for 30 min. Prior to each experiment, the electrodes were abraded with sandpaper to remove scale, treated with a solution of 10% HNO_3 in order to remove any previously deposited or adsorbed layers on the electrodes, washed with distilled water, dried, and weighed [43]. The electrodes were also weighed after each batch of test EC run with simulated wastewater at different current densities. The results show the increase in weight loss with the increase in values of current densities. After each batch during EC with real wastewater, samples were drawn periodically from the mixture. The pH was measured using a Denver Instrument UB-10 pH meter, and conductivity was measured using an Oakton CON 510 series conductivity meter.

2.2. Flow-through EC apparatus (FTECA)

A FTECA was supplied by Kaselco EC Treatment System, Texas. The FTECA essentially consists of a flow-through cell, the electrode assembly, a feed pump, and a DC power supply unit. A schematic diagram of the FTECA is shown in Fig. 2. The cell contained five parallel carbon steel (recycled steel, hot rolled, and not pickled) electrode plates (11.0 × 11.4 cm) placed 6.0 mm apart, which forms a four parallel cells. Before use, the plates were cleaned manually by abrading with sand papers. The internal volume of the cell is approximately 450 mL. A variable transformer or power supply was used to control the current and the applied potential [23].

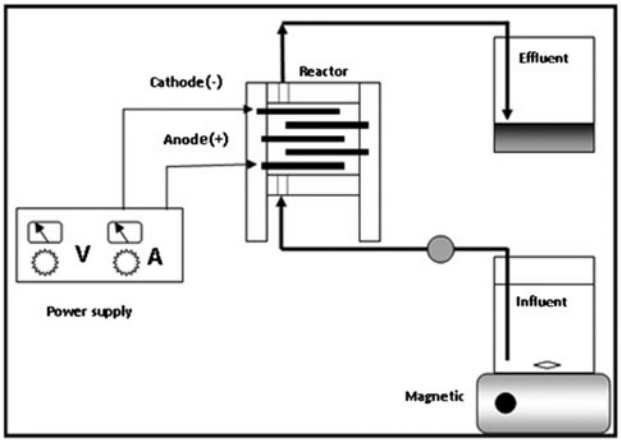


Fig. 2. Schematic of Kaselco bench reactor. *V* stands for voltmeter and *A* stands for ammeter.

In a typical EC experiment, the raw TWW was pumped through the FTEA at a predetermined flow rate (usually 500 mL/min), and after 2.5 L of the solution were treated the EC run was stopped. This constitutes one pass. The EC reactor is powered up for EC processes after the reactor is full with the wastewater. In one pass, 2-L treated water is obtained in 4 min. This 4 min of operating time can also be termed as EC interaction time as water and contaminants are in contact with the produced electrocoagulants for physico-chemical interaction during this period of time in every pass.

Using the conventional equation for residence time calculation (volume of the reactor/flow-rate), the residence time for each pass can be calculated as 54 s for the FTECA experiments. If the mixture is passed through the EC reactor again, it will make second pass, and so forth. After the completion of the EC runs, the floc was separated from the mixture using filter paper, and dried in vacuum desiccators at room temperature for performing further characterization, such as X-ray diffraction (XRD), scanning electron microscope-energy dispersive X-ray spectroscopy (SEM-EDS), Fourier transform-infrared spectrometer (FTIR) analyses. The filtrate was collected for analysis in atomic absorption spectrometer (AAS), inductively coupled Plasma-mass spectrometer (ICP-MS), ion chromatograph (IC), Dionex 1000, and Hach spectrophotometer-COD analyzer. ICP-MS data were obtained from an analytical company (Earth Analytical Sciences Inc., Beaumont, TX 77705). Ion Selective Electrode (ISE), Vernier was used to quantify nitrate and nitrite ions in TWW, and EC-treated water.

2.3. chemical oxygen demand (COD)

Hach DR-3000 spectrophotometer was used to measure the concentration of COD in the solution before and after the treatment. For measuring COD, the solution was digested in a reactor for 2 h before measuring the COD concentration.

The COD removal efficiency (% RE) was calculated from:

$$\% \text{ RE} = \left(\frac{C_0 - C}{C_0}\right) \times 100 \tag{14}$$

where C_0 is the initial COD concentration, and C is the final COD concentration.

2.4. Fourier transform infrared spectroscopy (FTIR)

FT-IR analysis were carried out by Thermo-electron Nexus 470 FT-IR spectrometer using potassium bromide pellets (usually, sample: KBr = 1:50). The spectra were recorded in the range of 4,000–400 with 4 cm^{-1} resolution. Twenty-five scans were averaged for each specimen.

2.5. Powder X-ray diffraction

The powder X-ray diffraction analysis of the EC-floc was carried out with a Bruker-AXS D8 Discover diffractometer with General Area Detector Diffraction System operating with a Cu K_α radiation source filtered with a graphic monochromator (λ = 1.5406 Å). The detector used was a HI-STAR two-dimensional multi-wire area detector. The EC-floc was dried overnight in the air, then ground to a fine powder, and loaded onto a double-sided scotch tape placed on a glass slide and mounted on a quarter-circle Eulerian cradle (Huber) stage. The X-ray beam was generated at 40 kV and 27 mA power, and was collimated to about 800 μm size of analysis spot on the sample. The incident ω angle was 5°. The laser/video system was used to ensure the alignment of the sample position on the instrument center. XRD scans were recorded from 7° to 77° of 2θ with 0.050 step-width, and 0.09 s step time. After running XRD on the samples, the data obtained were analyzed using DIFFRAC-Plus EVA program (Bruker AXS, Karlsruhe, Germany), and the patterns were identified using a computer reference database of ICDD PDF Maint.

2.6. Scanning electron microscope (SEM)

SEM (Hitachi S-3400N) with energy dispersive X-ray Spectrometer using EDAX detector was used to

Table 1
Composition of TWW, their MCL values regulated by U.S. EPA, and their concentrations in EC-treated water (this study). Post-treated water was obtained with flow through electrocoagulation apparatus using Fe-Fe electrodes at 2 mA/cm^2 current density

		Concentration (mg/L)		EPA	
Parameter	Instrumentation	Pre-treatment	Post-treatment	MCL(mg/L)	Removal (%)
Sodium	IC	231.5	219.9	–	5
Calcium	IC	6.01	1.497	–	75
Potassium	IC	4.08	3.538	–	13
Zinc	AAS	2.295	<0.0015	5	>99.9
Iron	AAS	5.63	<0.005	0.3	>99.9
Lead	ICP/MS	0.049	<0.005	0.015	>90
Cadmium	AAS	<0.008	<0.008	0.005	–
Chromium	ICP/MS	<0.003	<0.003	0.1	–
Nitrate	ISE	2.24	1.45	10	35
Nitrite	ISE	75.15	77.47	1	−3

investigate the morphology and the composition of the EC floc. The sample was spread onto a double-side carbon tape that was fixed on an aluminum tab.

2.7. Characteristics of truck wash water

Wastewater from truck wash facilities in general contains, petroleum products, hydrofluoric acid, ammonium bifluoride products, paint residues, rubber, phosphates, oil, grease, oil/water emulsion, sand and dust, carbon, asphalt, salts, surfactants, and organic matter, such as volatile organic compounds [2]. According to Fisheries and Oceans Department of Canada, the wash water produced by concrete deliver trucks has high value of pH (12), high turbidity (27,000 NTU), and total suspended solid (TSS) value of 79,000 ppm [44]. A Belgium study showed the range of car wastewater parameters for suspended solids (60–140 ppm), settable solids (1.0–6.0 mL/L), COD (208–51,000 ppm), BOD (63–9,620 ppm), pH (7.5–12.7), conductivity (0.7–286 mS/cm), non-ionic surfactants (32–13,000 ppm), anionic surfactants (0.7–42.6 ppm), and cationic surfactants (0.2–90 ppm) [4]. The wastewater that we used had the following characteristics: pH 6.3, conductivity: 1,070 mS/cm, TSS: 114 mg/L, total dissolved solid: 876 mg/L, chloride: 5 ppm, and oil and grease: under detection limit (<5.0 ppm). Other ionic concentration of metals, nitrate, and nitrite present in this wastewater are shown in Table 1.

3. Results and discussion

The collected TWW water from the truck wash center was very cloudy at the time of collection. After a few days, the sediment settled into the bottom of the tank. We used the apparently clear water from the top to treat for COD, metal cations, and a few anions.

Water samples were treated by EC with different combinations of electrodes such as Fe–Fe, Al–Fe, and Al–Al. The treated samples were then filtered with VWR grade filter paper (No. 410), and eventually tested for several cations and anions by AAS, IC, and ICP-MS. Conductivity and pH of the solution were recorded during the EC operation in both batch and FTECA methods. The pH of the reaction mixture was increased during EC run up to 11.4 for all combinations except for Al–Al combinations, where the pH went up to 9.3 while the initial pH was 6.3. Table 1 summarizes the results of before and after EC treatments for sodium, potassium, calcium, zinc, iron, cadmium, aluminum, chromium, and lead cations, and nitrate and nitrite anions. Higher removal efficiency was found for zinc (>99.9%), iron (>99.9%), and calcium (75%). They are all divalent cations except iron that has also trivalency. The concentration of monovalent cations, such as sodium (5%) and potassium (13%), was slightly decreased. The efficiency of lead removal was 90%. The concentration of cadmium, aluminum, and chromium was found under detection limit in the raw TWW water. The concentration of nitrate was decreased by 35%, whereas the concentration of nitrite was increased by 3% after EC treatment. There might be a possibility that during EC nitrates were partially reduced to nitrites [45]. Nitrites might be also generated from electrochemical degradation of nitrogen containing organic species, such as detergents and lubricants that are present in the TWW [46].

3.1. Removal of heavy metals

Experiments were performed to find the concentration of several environmentally significant metalloid/heavy metals such as arsenic, iron, zinc, lead, chromium, cadmium, and aluminum before and after the EC-treatment. The sample concentration, after EC-treatment, was found to be below the detection limit in raw water. Arsenic, chromium, and cadmium, and aluminum were also found under detection limit in EC-treated water. The highest concentration of zinc found in the solution was 2.3 mg/L (below MCL), and was removed successfully (>99%) from the water by EC after 4 min of operating time in the EC reactor. Iron concentration in the TWW solution was 5.62 mg/L. After 4 min of Fe–Fe EC run, the removal efficiency was 94%, which had been increased to more than 99% in second pass (8 min) of FTECA. Similar removal efficiencies of iron were found for other combination of electrodes in EC.

Treatment with aluminum electrode introduced aluminum into the treated water. This inclusion possibly occurs due to dissolution of aluminum during electro-oxidation, and incomplete removal of soluble Al^{3+} through their physico-chemical interaction with floc materials. The ultimate concentration was found to be 0.05 ppm. Table 1 shows a comparison between the MCL of some metals and the concentrations of those metals found after EC run. This indicates the effectiveness of EC for complying EPA regulations for most of those metals present in TWW.

3.2. COD Removal

Raw and treated truck wash wastewater samples were investigated to observe COD removal efficiency through EC. Table 2 shows the measured data for pH, conductivity, and COD at different operating time during EC with Fe–Fe, Fe–Al, and Al–Al electrode pairs.

As shown in Table 2, 80% of COD was removed by Fe–Fe electrode at 2.0 mA/cm^2 current density (CD) after two passes, where the pH was changed from 6.2 to 7.4. Similarly, for Al–Fe electrode pair, 52% of COD was removed at 11.1 mA/cm^2 CD after 4 min of operating time, where the pH was changed from 7.2 to 8.5. For Al–Al electrode pair, 69% of COD was removed at 2.0 mA/cm^2 CD after 4 min of operating time, where the pH was changed from 7.0 to 7.2. According to Pourbaix [47], although the pH of the EC reaction mixture and the applied potential plays an important role on the precipitation/solubility of metal oxides/hydroxides/oxyhydroxides, simultaneous variation of EC parameters, such as amount of

Table 2
Measured data for pH, conductivity and COD at different operating time during electrocoagulation with Fe–Fe, Fe–Al, and Al–Al electrode pairs

Electrode Pair ↓	Current density (mA /cm^2)	0			4			8			12			16			
Time (min)→		pH	Conductivity (mS)	COD ppm	pH	Conductivity (mS)	COD ppm	pH	Conductivity (mS)	COD ppm	pH	Conductivity (mS)	COD ppm	pH	Conductivity (mS)	COD ppm
Fe–Fe	2.0	6.2	3.2	260	7.1	3.2	90	7.4	3.0	54	9.6	2.8	54	10.8	3.4	78
Fe–Fe	3.2	6.4	3.2	398	8.2	3.3	225	8.7	3.4	160	9.2	3.3	180	9.8	3.4	164
Fe–Fe	8.0	7.3	3.1	260	11.1	3.2	156	11.6	3.3	143	10.2	3.2	137	10.0	3.3	168
Fe–Fe	11.1	6.1	1.1	398	9.3	1.0	160	10.4	1.1	107	11.0	1.2	100	11.4	1.3	99
Fe–Fe	16.0	6.9	2.8	160	10.2	2.9	148	10.1	3.0	135	10.2	3.1	130	12.0	3.2	146
Fe–Al	2.0	7.0	2.7	260	8.0	2.7	140	8.1	2.7	135	8.2	2.7	146	8.3	2.7	158
Fe–Al	3.2	6.9	2.8	260	7.9	2.8	140	8.0	2.8	144	8.3	2.8	170	8.3	2.8	135
Fe–Al	8.0	7.0	3.1	260	8.0	3.2	154	8.0	3.2	169	8.9	3.2	155	8.4	3.2	140
Fe–Al	11.1	7.2	1.0	260	8.5	1.0	126	9.5	1.0	139	10.0	1.0	133	10.0	1.0	131
Fe–Al	16.0	7.5	1.0	160	8.9	1.1	172	9.8	1.0	173	9.3	1.0	176	9.9	1.0	175
Al–Al	2.0	7.0	3.2	260	7.2	3.4	80	7.7	3.4	88	7.9	3.4	89	8.0	3.4	114
Al–Al	3.2	6.0	2.6	260	6.8	2.5	126	7.3	2.5	190	7.9	2.5	235	8.1	2.7	275
Al–Al	8.0	6.0	2.5	260	7.7	2.6	254	8.1	2.9	230	8.2	3.0	167	8.3	3.1	160
Al–Al	11.1	7.4	2.6	260	8.1	2.8	210	8.2	3.0	184	8.3	3.2	140	8.4	3.4	200
Al–Al	16.0	7.0	2.7	260	8.0	2.7	206	8.2	2.9	189	8.4	3.5	204	8.5	3.8	214

produced oxidizable species, does not help us make one to one correlation among COD removal and EC variables. Therefore, we could only make general statement on the results.

Fig. 3 shows the removal of COD in variable current densities using Fe–Fe electrode pairs. The initial and final COD concentrations after second EC pass at 2.0 mA/cm^2 CD were 260 and 54 ppm, respectively. According to Fig. 3, the increase in CD rendered lower removal efficiency for all cases except for 11.2 mA/cm^2. The eventual increases in EC cycles or passes affect removal efficiency negatively after second or third pass. COD removal efficiencies showed a linear increase up to second full pass. From second to third EC pass, there was no significant fluctuation in the results. In contrast, at fourth EC pass, the removal efficiency started to slowly decrease. The best removal efficiency has been achieved at second pass at CD of 2.0 mA/cm^2, while the lowest was obtained at 16.0 mA/cm^2.

COD removal efficiency depends not only on the removal of COD components present in the TWW water, but also on the addition of oxidizable species to the treated water through electrochemical reactions during EC. With the increase in CD and no. of passes, more Fe(II) ions are produced. The increase in oxidizable Fe(II) ions incorporates additional Chemical Oxidation Demand values. As mentioned earlier, GR is mainly responsible for the removal of COD, although other species, such as iron oxides, hydroxides, and oxyhydroxides may have minor contribution to the final removal values. It was experimentally observed by Moreno et al. [48] that the pH in between 7 and 9 is probably more favorable for GR formation as shown in Fig. 4, as it needs both Fe(II) and Fe(III) hydroxides

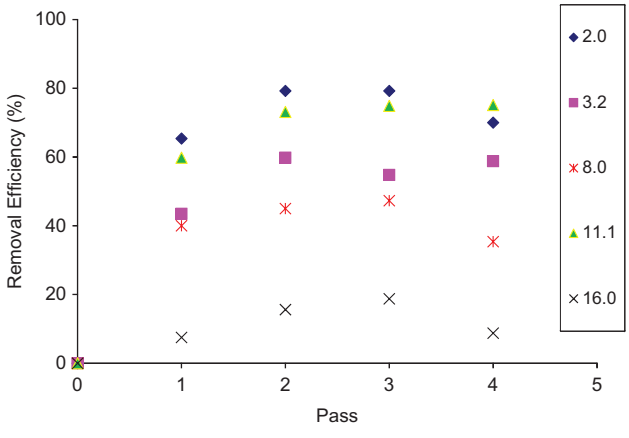


Fig. 3. Removal of COD from Raw TWW with Fe–Fe electrode (FTECA) at different CD (mA/cm^2). The legend shows the values of different CD values.

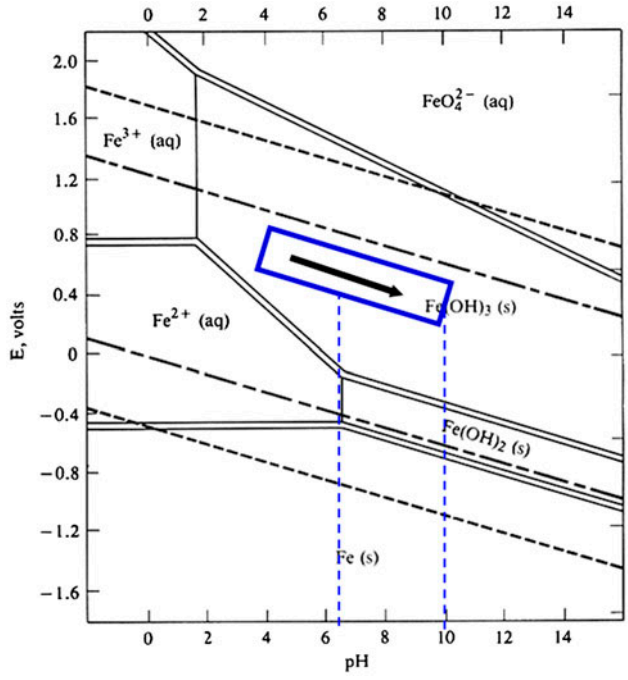


Fig. 4. Pourbaix diagram showing the favorable region for GR formation [47,48].

as shown in Formula (9). Fig. 5 shows the variation of final pH after each pass at different current densities with Fe–Fe EC of this work, and it generally agrees with that of Moreno et al. [48]. One needs to consider both the thermodynamic aspect [47] and GR formation aspect to understand the COD removal, or in general removal of water contaminants in EC. Sometimes, with the changes of other environmental parameters, the explanation of the trends becomes more tedious. For example, with the increase of operating time, the previously produced GR might oxidize to other compounds, such as Fe_2O_3 that might have lower capacity of COD removal as compared to GR. A decrease in COD removal efficiency at higher passes or at higher CD might be related either to increased amount of newly formed Fe(II), or insignificant formation of GR.

Results from Al–Fe electrode combinations were demonstrated in Fig. 6. As Fig. 6 shows, the highest removal (52%) was found at CD of 11.1 mA/cm^2 after first EC pass. Since at lower CD, enough flocs are not produced compared to higher values, it might cause to produce lower removal efficiency at lower values of CD.

In the combination of Al Fe electrodes, aluminum was inserted as bipolar electrodes in between Fe electrodes in the electrode assembly. In case of Al–Fe combination, with the change of operating time, pH may have significant impact on the removal efficiency.

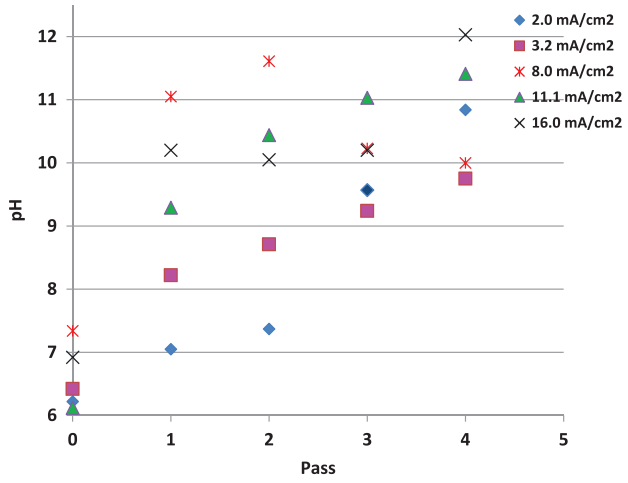


Fig. 5. Variation of pH with EC-passes at different CD using Fe–Fe EC.

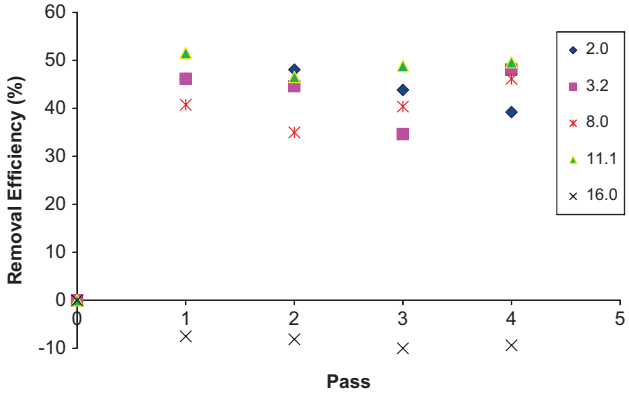


Fig. 6. Removal of COD by Al–Fe electrode (FTECA) at different CD (mA/cm^2). The legend shows the values of different CD values.

At the CD of 2 mA/cm^2, the pH of treated water was changed to 8.1 after the end of second EC pass. But, in case of the CD of 3.2 mA/cm^2, the pH reached up to 7.9 after first pass. According to the Pourbaix diagram of water–aluminum system [47], aluminum stays in passivated form by forming oxides or hydroxides near the pH 4–8. Solubility of aluminum is also lowest around pH 6–7, and goes upward at both the ends of this pH range. Since, at lower current densities, the final pH stays near to 8, one may conclude that at lower current densities, fewer amount of soluble aluminum ions are present in the aqueous form, and higher amounts of floc are produced. At higher current densities, pH of the mixture reached a value greater than the passivation area as mentioned by Pourbaix [47] indicating increased corrosion of aluminum through formation of soluble AlO_2^{2-} and decreased formation of floc. This increase in pH is also occurred with the increase of EC passes. This explains the lower removal COD efficiency with the increase in EC run. On the other hand, formation of iron oxides/hydroxides is thermodynamically more favorable at higher pH as observed in the Pourbaix diagram of iron–water system [47]. All these compensates to the formation of more aluminum substituted iron oxide/hydroxide floc [49], and thus better removal of COD at higher CD (11.1 mA/cm^2) in the case of Al–Fe combinations. The COD of treated TWW at 16 mA/cm^2 did not reduce, rather increased. This may possibly happen due to higher production of oxidizable species, such as Fe(II), and formation of less modified GR [50] when compared to experiments with other current densities.

Like EC treatment with Fe–Fe and Al–Fe combination electrode assembly, Al–Al combinations also showed the highest removal efficiency of about 70% at CD of 2.0 mA/cm^2 (Fig. 7). An increase in the operating time or EC passes did not have a significant impact on the removal efficiency. The increase in current in fact resulted in lower removal efficiency. As CD increases pH of the solution increases due to the production of more hydroxide ions at the anode. Similarly, multiple passes also increase pH of the solution due to prolonged amount of electric charge flowed through the EC reactor. As discussed earlier, higher pH brings more soluble aluminum ions in the system, thereby reducing the amount of aluminum floc required for COD removal. The increase in removal efficiency up to 30–40% with the increase in number of passes at higher CD (11.1–16.0 mA/cm^2) might simply indicate the cumulative removal effects of COD during every additional pass.

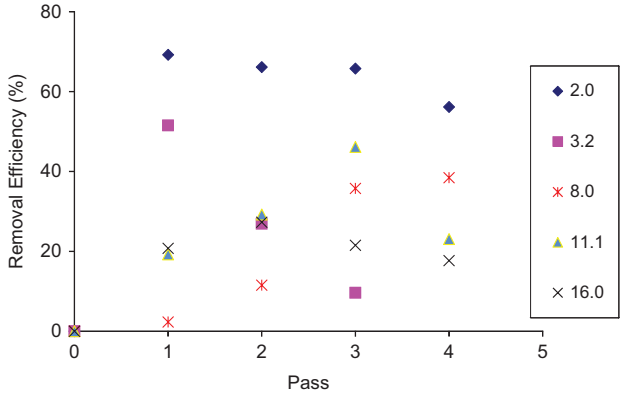


Fig. 7. Removal of COD by Al–Al electrode (FTECA) at different CD (mA/cm^2). The legend shows the values of different CD values.

3.3. Characterization of EC-Floc: FTIR

FT-IR spectrum of floc produced Al–Al electrode assembly (Fig. 8, Al–Al electrodes) shows Al–O-H bending at 1,638 cm^{-1}. Floc from Fe–Fe electrode assembly (Fig. 8, Fe–Fe electrodes) also showed hydroxyl (OH) bending and HO–H_2O bending vibration, or overtones of hydroxyl bending around 1,637 cm^{-1} [49]. FT-IR analysis of the floc obtained from Al–Fe electrode assembly suggested the presence of hydroxyl bending and HO–H_2O bending vibration or overtones of hydroxyl bending around 1,637 cm^{-1}. The higher absorbance for OH, and HO–H_2O vibrations for Fe–Fe in compared to Al–Fe, and Al–Al systems, signifies that more species with these moieties are present for the case of Fe–Fe system. The stretching band of OH was identified around 3,400 cm^{-1} [49] for all three systems including the blue shift for the case of Al–Al system compared to others. This OH might be a part of iron/aluminum hydroxides or oxyhydroxide.

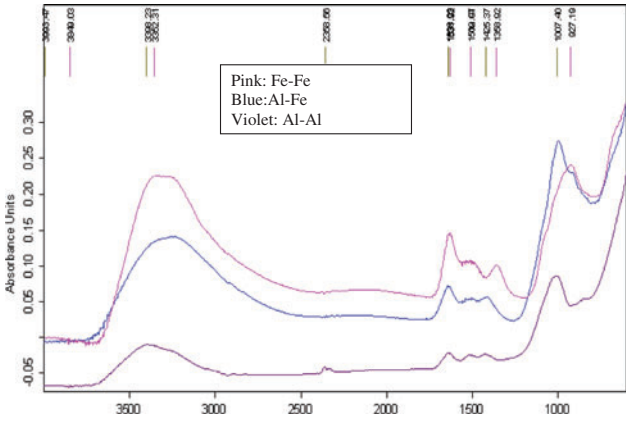


Fig. 8. FT-IR spectra of the solid EC by-products using Al–Fe, Fe–Fe, and Al–Al electrode combinations. *X*-axis indicates the wave number (cm^{-1}), and *y*-axis indicates absorbance units. The identified wave numbers in the top of the image are from left to right: 3,993.47, 3,849.03, 3,398.23, 3,352.31, 2,358.56, 1,638.23 (merged), 1,508.47 (merged), 1,425.37, 1,358.92, 1,007.40, and 927.19.

3.4. X-ray diffraction (XRD)

Flocs originated from Fe–Fe electrode combination shows well crystalline phases of magnetite, and the poorly crystalline phases of iron oxyhydroxides, such as lepidocrocite (Fig. 9(A)). The presence of poorly crystalline phases of iron oxyhydroxides were verified from the FT-IR analysis of the floc of this Fe–Fe system (Fig. 8).

XRD pattern of the floc from Al–Al electrode combination (Fig. 9(C)) showed very broad and shallow diffraction peaks. Bragg reflections possessing very broad humps and low intensity indicate that the analyzed phase possesses a short-range order, i.e.

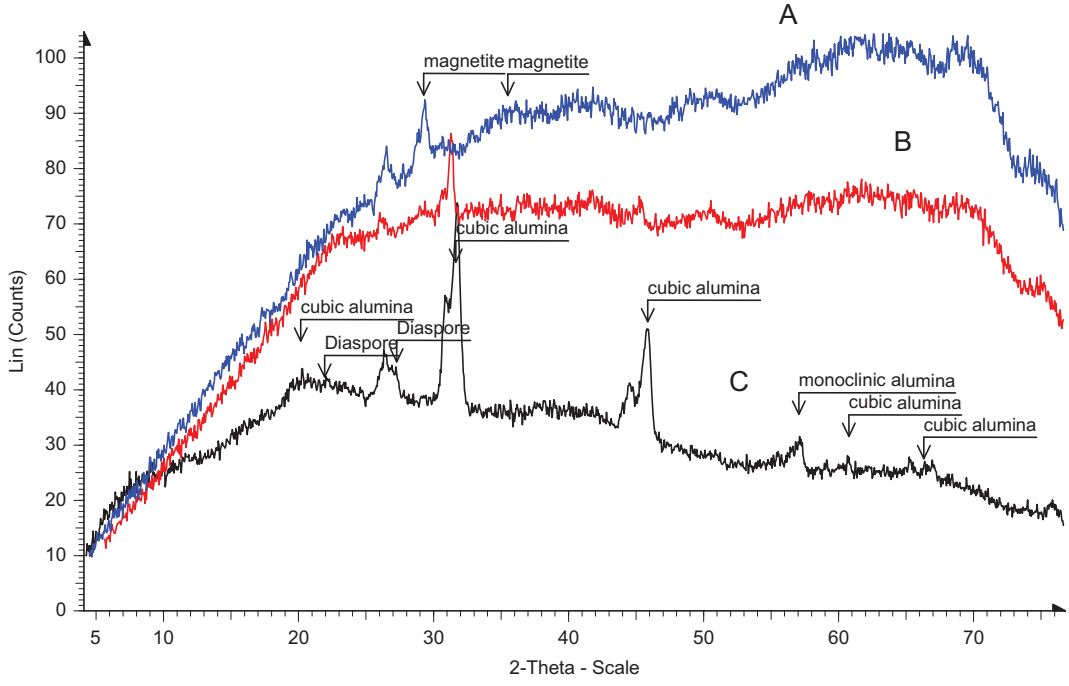


Fig. 9. XRD pattern of the EC-floc obtained after EC run (the top blue pattern (A) points to EC-floc with Fe–Fe, the middle red pattern (B) with Al–Fe, and the bottom black pattern (C) is with Al–Al electrode combinations).

amorphous or very poorly crystalline in nature. Fig. 9(C) shows broad peaks of alumina and diaspore (Al–O–OH).

From FT-IR and XRD analyses of the floc from Al–Fe electrode combination (Figs. 8 and 9), it can be concluded that the chemical speciation of this amorphous phase can be aluminum hydroxide and/or aluminum oxyhydroxide. Because crystallization of Al hydroxides/oxyhydroxides is a very slow process, most Al hydroxides and aluminum oxyhydroxides found to be either amorphous or very poorly crystalline [49]. Fig. 9(B) shows the shifted alumina peak by about 1° (2-theta) and a suppressed peak of magnetite compared to Fig. 9(A), which confirms the isomorphous substitution of Al^{3+} for Fe^{3+} in iron oxides [49].

3.5. scanning electron microscope-energy dispersive X-ray spectroscopy (SEM-EDS)

The SEM image of the floc obtained after EC with Fe–Fe electrode system indicates the micrometer sized particles over the cracked surface. The EDS calculation shows the presence of Fe (57.0 At%), O (28.0 At%), Ca (4.2 At%), Na (0.7 At%), Mg (0.4 At%), Al (2.4 At%), Si (4.8 At%), and P (2.7 At%) on the floc. Si, P, Na, Al, Ca, and Mg may originate from the truck wash waste.

The SEM image of the floc obtained after EC with Al–Al electrode system appears to be of spongy-type of several micrometer size (Fig. 10). The EDS re-calculation indicates the presents of Al (10.0 At%), O (37.4 At%), Ca (1.3 At%), Na (17.7 At%), F (1.3 At%), Cl (28.6 At%), Si (1.3 At%), and P (1.7 At%) in the floc. Similarly, Si, P, Na, Ca, F, and Cl may originate from the truck wash waste.

In Summary, EC can efficiently remove toxic metals present in TWW, and make it in compliance with EPA MCLs. It can also considerably carve COD indicating removal of oxidizable species present in TWW. Consequently, the treated water can be reused in the same facility. This is definitely a step to prevail over water shortage and to sustain the environment.

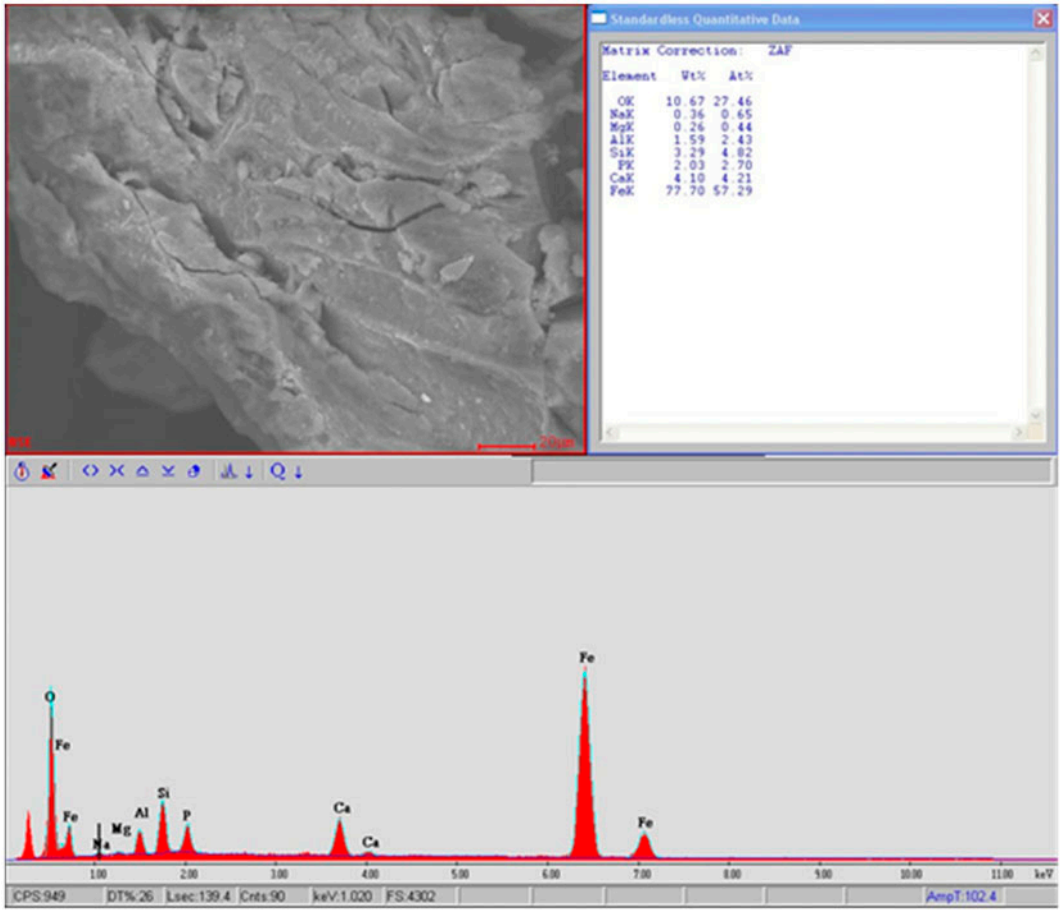


Fig. 10. SEM image of the EC-byproducts originated in the Fe–Fe electrode system after fourth EC pass at 16.0 mA/cm^2. *X*-axis indicates energy level in eV (0–11.5), and *y*-axis indicates the generated X-ray counts.

Acknowledgment

We are grateful to Welch foundation (V-1103), ATP (003581-0033-2003), and USDA (2004-38899-02181) for their financial support for this research. We are thankful to Kaselco, Mr Ashik Mahmud, and Mr Jaime Bazan for their support to use their facilities and instrumentation, and to Lamar University MIC and Mr Dan Rutman for generating SEM-EDS images.

References

[1] Research and Innovation Technology Administration, Bureau of Transportation Statistics, 2008. Available from: <http://www.bts.gov/publications/national_transportation_statistics/html/table_01_11.html>.
[2] Z.A. Bhatti, Q. Mahmood, I.A. Raja, A.H. Malik, M.S. Khan, D. Wu, Chemical oxidation of carwash industry wastewater as an effort to decrease water pollution, Phys. Chem. Earth Parts A/B/C 36 (2011) 465–469.
[3] A. Al-Odwani, M. Ahmed, S. Bou-Hamad, Carwash water reclamation in Kuwait, Desalination 206 (2007) 17–28.
[4] K. Boussu, C. Kindts, C. Vandecasteele, B.V.d. Bruggen, Applicability of nanofiltration in the carwash industry, Sep. Purif. Technol. 54 (2007) 139–146.
[5] A. Seidel, J.J. Waypa, M. Elimelech, Role of charge (Donnan) exclusion in removal of arsenic from water by a negatively charged porous nanofiltration membrane, Environ. Eng. Sci. 18 (2001) 105–113.
[6] A. Katsoyiannis, A.I. Zouboulis, Application of biological processes for the removal of arsenic from groundwaters, Water Res. 38 (2004) 17–26.
[7] J. Kim, M.M. Benjamin, Modeling a novel ion exchange process for arsenic and nitrate removal, Water Res. 38 (2004) 2053–2062.
[8] K.N. Ghimire, K. Inoue, H. Yamaguchi, K. Makino, M. Tohru, Adsorptive separation of arsenate and arsenite anions from aqueous medium by using orange waste, Water Res. 37 (2003) 4945–4953.
[9] J.A. Jay, N.K. Blute, H.F. Hemond, J.L. Durant, Arsenic-sulfides confound anion exchange resin speciation of aqueous arsenic, Water Res. 38 (2004) 1155–1158.
[10] K.V. Hege, M. Verhaege, W. Verstraete, Electro-oxidative abatement of low-salinity reverse osmosis membrane concentrates, Water Res. 38 (2004) 1550–1558.
[11] N. Balasubramanian, K. Madhavan, Arsenic removal from industrial effluent through electrocoagulation, Chem. Eng. Technol. 24 (2001) 519–521.
[12] J.R. Parga, D.L. Cocke, J.L. Valenzuela, J.A. Gomes, M. Kesmez, G. Irwin, H. Moreno, M. Weir, Arsenic removal via electrocoagulation from heavy metal contaminated groundwater in La Comarca Lagunera México, J. Hazard. Mater. 124 (2005) 247–254.
[13] M.Y.A. Mollah, P. Morkovsky, J.A.G. Gomes, M. Kesmez, J. Parga, D.L. Cocke, Fundamentals, present and future perspectives of electrocoagulation, J. Hazard. Mater. 114 (1–3) (2004) 199–210.
[14] N. Adhoum, L. Monser, N. Bellakhal, J.-E. Belgaied, Treatment of electroplating wastewater containing Cu^{2+}, Zn^{2+} and Cr(VI) by electrocoagulation, J. Hazard. Mater. 112 (2004) 207–213.
[15] X. Xu, X. Zhu, Treatment of refectory oily wastewater by electro-coagulation process, Chemosphere 56 (2004) 889–894.
[16] H. Inan, A. Dimoglo, H. Şimşek, M. Karpuzcu, Olive oil mill wastewater treatment by means of electro-coagulation, Sep. Purif. Technol. 36 (2004) 23–31.
[17] R.R. Babu, N.S. Bhadrinarayana, K.M. Meera, S. Begum, N. Anantharaman, Treatment of tannery wastewater by electrocoagulation, J. Univ. Chem. Technol. Metall. 42 (2007) 201–206.
[18] J.A.G. Gomes, D. Atambo, K.K. Das, G. Irwin, H. Moreno, D.L. Cocke, Remediation of chicken processing wastewater using electrochemically produced layered double hydroxides, in: E.V. Edgar, A. Hagni, L.F. Michael, N.A. Prince (Eds.), Supplement Proceedings: Vol. 2: Materials Characterization, Computation, Modeling and Engergy, 139th TMS Annual Meeting and Exhibition, February 14–18, Seattle, WA, 2010, pp. 541–547.
[19] J. Gomes, D. Cocke, K. Das, M. Guttula, D. Tran, J. Beckman, Treatment of produced water By electrocoagulation, in: M.H. Stanley, N.A. Prince, Z. Lifeng (Eds.), Proceedings of TMS 138th Annual Meeting, February 15–19, San Francisco, CA, 2009, pp. 459–466.
[20] M.F. Pouet, A. Grasmick, Urban wastewater treatment by electrocoagulation and flotation, Water Sci. Technol. 31 (1995) 275–283.
[21] X. Chen, G. Chen, P.L. Yue, Separation of pollutants from restaurant wastewater by electrocoagulation, Sep. Purif. Technol. 19 (2000) 65–76.
[22] Y.A.M. Mollah, S.R. Pathak, P.K. Patil, M. Vayuvegula, T.S. Agrawal, J.A.G. Gomes, M. Kesmez, D.L. Cocke, Treatment of orange II azo-dye by electrocoagulation (EC) technique in a continuous flow cell using sacrificial iron electrodes, J. Hazard. Mater. 109 (2004) 165–171.
[23] Y.A.M. Mollah, J.A.G. Gomes, K.K. Das, D.L. Cocke, Electrochemical treatment of Orange II dye solution—Use of aluminum sacrificial electrodes and floc characterization, J. Hazard. Mater. 174 (2010) 851–858.
[24] M. Kobya, F. Ulu, U. Gebologlu, E. Demirbas, M.S. Oncel, Treatment of potable water containing low concentration of arsenic with electrocoagulation: Different connection modes and Fe–Al electrodes, Sep. Purif. Technol. 77 (2011) 283–293.
[25] E. Lacasa, P. Cañizares, C. Sáez, F.J. Fernández, M.A. Rodrigo, Removal of nitrates from groundwater by electrocoagulation, Chem. Eng. J. 171 (2011) 1012–1017.
[26] M.M. Emamjomeh, M. Sivakumar, Fluoride removal by a continuous flow electrocoagulation reactor, J. Environ. Manage. 90 (2009) 1204–1212.
[27] M.F. Ni'am, F. Othman, J. Sohaili, Z. Fauzia, Removal of COD and turbidity to improve wastewater quality using electrocoagulation technique, Malays. J. Anal. Sci. 11 (2007) 198-205.
[28] D. Jolis, R.A. Hirano, P.A. Pitt, A. Müller, D. Mamais, Assessment of tertiary treatment technology for water reclamation in San Francisco, California, Water Sci. Technol. 33 (1996) 181–192.
[29] R.A. Mills, T. Asano, A retrospective assessment of water reclamation projects, Water Sci. Technol. 33 (1996) 59–70.
[30] J. Crook, R.Y. Surampalli, Water reclamation and reuse criteria in the US, Water Sci. Technol. 33 (1996) 451–462.

[31] D. Norton-Brandão, S.M. Scherrenberg, J.B.v. Lier, Reclamation of used urban waters for irrigation purposes—A review of treatment technologies, J. Environ. Manage. 122 (2013) 85–98.
[32] T. Cazurra, Water reuse of south Barcelona's wastewater reclamation plan, Desalination 218 (2008) 43–51.
[33] P. Sipos, D. Zeller, E. Kuzmann, A. Vértes, Z. Homonnay, M. Walczak, S.E. Canton, The structure of Fe(III) ions in strongly alkaline aqueous solutions from EXAFS and Mossbauer spectroscopy, Dalton Trans. (2008) 5603–5611.
[34] H.A. De Abreu, L. Guimarães, H.A. Duarte, Density-functional theory study of iron(III) hydrolysis in aqueous solution, J. Phys. Chem. A 110(24) (2006) 7713–7718.
[35] H.K. Hansen, P. Nu˜nez, D. Raboy, I. Schippacasse, R. Grandon, Electrocoagulation in wastewater containing arsenic: Comparing different process designs, Electrochim. Acta 52 (2007) 3464–3470.
[36] A.G.B. Williams, M.M. Scherer, Kinetics of Cr(VI) reduction by carbonate green rust, Environ. Sci. Technol. 35 (2001) 3488–3494.
[37] H.C.B. Hansen, C.B. Koch, H. Nancke-Krogh, O.K. Borggaard, J. Sørensen, Abiotic nitrate reduction to ammonium: Key role of green rust, Environ. Sci. Technol. 30(6) (1996) 2053–2056.
[38] D. Krawczyk, Water Quality Parameters, National Environmental Research Center, ASTM, Philadelphia, PA, 1975, pp. 152–163.
[39] M. Kobya, A. Akyol, E. Demirbas, M.S. Oncel, Removal of arsenic from drinking water by batch and continuous electrocoagulation processes using hybrid Al-Fe plate electrodes, Environ. Prog. Sustainable Energy 33 (2013) 131–140.
[40] R. Katal, H. Pahlavanzadeh, Influence of different combinations of aluminium and iron electrode on electrocoagulation efficiency: Application to the treatment of paper mill wastewater, Desalination 265 (2011) 199–205.
[41] Y. Yavuz, E. Öcal, A.S. Koparal, Ülker Bakır Öğütveren, Treatment of dairy industry wastewater by EC and EF processes using hybrid Fe–Al plate electrodes, J. Chem. Technol. Biotechnol. 86 (2011) 964–969.
[42] C.L. Lai, S.H. Lin, Electrocoagulation of chemical mechanical polishing (CMP) wastewater from semiconductor fabrication, Chem. Eng. J. 95 (2003) 205–211.
[43] M.G. Arroyo, V. Pérez-Herranz, M.T. Monta˜nés, J. García-Antón, J.L. Guiñón, Effect of pH and chloride concentration on the removal of hexavalent chromium, J. Hazard. Mater. 169 (2009) 1127–1133.
[44] Fisheries and Oceans Canada. Available from: <http://www-heb.pac.dfo-mpo.gc.ca/water_quality/fish_and_pollution/conc_char_e.htm> (accessed on 27 May 2014).
[45] M. Paidar, I. Rouser, K. Bouzek, Electrochemical removal of nitrate ions in waste solutions after regeneration of ion exchange columns, J. Appl. Electrochem. 29 (1999) 611–617.
[46] J.P. Coates, L.C. Setti, Infrared spectroscopic methods for the study of lubricant oxidation products, ASLE Trans. 29 (1986) 394–401.
[47] M. Pourbaix, Atlas of Electrochemical Equilibria in Aqueous Solutions, National Association of Corrosion Engineers, Houston, TX, 1974.
[48] A. Hector, C. Moreno, D.L. Cocke, J.A.G. Gomes, P. Morkovsky, J.R. Parga, E. Peterson, C. Garcia, Electrochemical reactions for electrocoagulation using iron electrodes, Ind. Eng. Chem. Res. 48(4) (2009) 2275–2282.
[49] J.A.G. Gomes, P. Daida, M. Kesmez, M. Weir, H. Moreno, J.R. Parga, G. Irwin, H. McWhinney, T. Grady, E. Peterson, D.L. Cocke, Arsenic removal by electrocoagulation using combined Al–Fe electrode system and characterization of products, J. Hazard. Mater. 139 (2007) 220–231.
[50] A.J. Gomes, A. Baksi, I. Haider, J. Gossage, H. Moreno, D. Cocke, Electrochemical generation of green rust and modified green rust for water treatment applications, Curr. Inorg. Chem. (accepted proofs) 6(2) (2016) in press.